Computational Conformal Geometry Applied in Engineering Fields

Article

4 authors, including:

Xianfeng David Gu
Stony Brook University
374 PUBLICATIONS **6,402** CITATIONS
SEE PROFILE

Miao Jin
University of Louisiana at Lafayette
69 PUBLICATIONS **1,354** CITATIONS
SEE PROFILE

ICCM 2007 · Vol. II · 72–94

Computational Conformal Geometry Applied in Engineering Fields

Xianfeng Gu, Miao Jin, Junho Kim [*], Shing-Tung Yau[†]

Abstract

Computational conformal geometry is an interdisciplinary field, combining modern geometry theories from pure mathematics with computational algorithms from computer science. Computational conformal geometry offers many powerful tools to handle a broad range of geometric problems in engineering fields. This work summarizes our research results in the past years. We have introduced efficient and robust algorithms for computing conformal structures of surfaces acquired from the real life, which are based on harmonic maps, holomorphic differential forms and surface Ricci flow. We have applied conformal geometric algorithms in computer graphics, computer vision, geometric modeling and medical imaging.

2000 Mathematics Subject Classification: 20C30, 20J05.
Keywords and Phrases: Cohomology, Symmetric group, Rotation group.

1 Introduction

Computational conformal geometry is an interdisciplinary field, combining modern geometry theories from pure mathematics with computational algorithms from computer science.

From theoretical point of view, computational conformal geometry has deep roots in mathematics and physics. In mathematics, it is the intersection of many fields, such as algebraic topology, differential geometry, Riemann surface, harmonic analysis, and so on. It also has close relation with many physics fields, such as electromagnet field in electrodynamics, elasticity deformation in mechanics, heat diffusion in thermal dynamics, modular space theory in super string theory.

From practical point of view, computational conformal geometry offers many powerful tools to handle a broad range of geometric problems in engineering world.

Recently, the 3*D* scanning technology is developing extremely fast. Figure 1 shows several facial surfaces with different expressions of the same person, which are scanned

[*]X. Gu, M. Jin and J. Kim are with the Department of Computer Science, State University of New York at Stony Brook, Stony Brook, New York 11794-4400, USA.
{E-mail:gu,mjin,jkim}@cs.sunysb.edu.
[†]S.-T. Yau is with the Mathematics Department, Harvard University, Boston, MA 02138, USA.
This work is supported by National Science Foundation of USA.

Figure 1 Face geometries with different expressions of the same person, scanned using real time high speed high resolution scanner.

by a scanner based on the phase-shifting method [1]. The scanning speed is as fast as 180 frames per second, each frame has 640×480 samples. The scanner can capture dynamic facial expressions in real time. It is challenging to process the huge amount geometric data efficiently and robustly especially in real time.

The basic geometric processing tasks include shape representation, geometric compression, surface repairing, shape de-noise and smoothing, surface stitching and merging, meshing and re-meshing, mesh and spline conversion. High level shape operations include surface classification, shape comparison, surface matching and recognition, shape manipulation, and many others.

Computational conformal geometric methods can handle most of the above tasks directly or indirectly. The main strategy is to use conformal mappings to transform $3D$ surfaces to canonical $2D$ domains, and convert $3D$ geometric problems to $2D$ ones.

Figure 2 Visualization of a holomorphic differential form on the bunny surface.

2 Theoretic background

Conformal geometry studies the *conformal structure* of general surfaces. Conformal structure is a natural structure of all surfaces in real life. Riemannian metric is a structure to measure the lengths of curves on the surface, the areas of domains on the surface and the intersection angles between curves. Conformal structure is a structure to only measure the intersection angle between two curves on the surface.

A complex function $f : \mathbb{C} \to \mathbb{C}, (x,y) \to (u,v)$ is called *holomorphic*, if it satisfies the following Riemann-Cauchy equation

$$\frac{\partial u}{\partial x} = \frac{\partial v}{\partial y}, \frac{\partial u}{\partial y} = -\frac{\partial v}{\partial x}.$$

Suppose S is a topological 2-manifold with an atlas $\mathscr{A} = \{(U_\alpha, \phi_\alpha)\}$, such that all the coordinates transition functions are holomorphic, then S is called a *Riemann surface*. $\mathscr{A}$ is called a *conformal atlas*. The maximal conformal atlas is called a *conformal structure* of S.

Suppose S_1 and S_2 are two Riemann surfaces, $\phi : S_1 \to S_2$ is a mapping between them. Suppose (U_α, ϕ_α) is a local chart of S_1 and (V_β, ψ_β) is a local chart of S_2, then if the local presentation of ϕ, $\psi_\beta \circ \phi \circ \phi_\alpha^{-1}$, is always holomorphic, then we say ϕ is a *holomorphic map* or *conformal map*. A *conformal map* between two surfaces preserves angles.

2.1 Riemann mapping

Riemann mapping theorem states that any simply connected surface with a single boundary (a topological disk) can be conformally mapped to the unit disk. As shown in figure 3, a human face S is a topological disk and mapped to the unit disk $\mathbb{D}$ by a conformal mapping $\phi : S \to \mathbb{D}$. Suppose γ_1, γ_2 are two arbitrary curves on the face surface S, ϕ maps them to $\phi(\gamma_1), \phi(\gamma_2)$. If the intersection angle between γ_1, γ_2 is θ, then the intersection angle between $\phi(\gamma_1)$ and $\phi(\gamma_2)$ is also θ. γ_1 and γ_2 can be chosen arbitrarily. Therefore, we say ϕ is *conformal*, meaning *angle-preserving*.

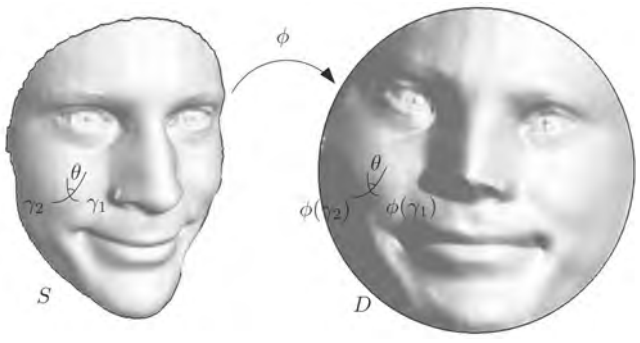

Figure 3 A Riemann mapping from a human face to the unit disk, the mapping is angle-preserving.

The conformality can be visualized using *texture mapping* techniques in computer graphics. Figure 4 illustrates the idea. A texture refers to an image on the plane. First a conformal mapping between the face surface (a) to the unit disk is established. Then we cover the disk by a texture image, pull back the image onto the surface. In this way, the mapping can be directly visualized. If the texture is a checker board, then the pull back map glues the checker board to the face surface. Because the map is conformal, all the right angles of the corners of the checkers are preserved on the face as shown in (b). If we replace the texture by a circle packing pattern, then planar circles are mapped to circles on the surface, the tangency relation among circles are preserved as shown in (c).

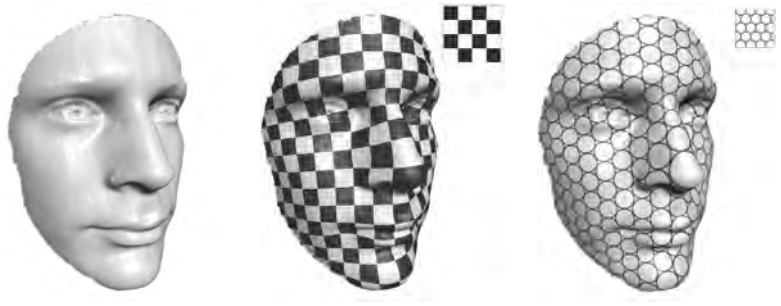

(a)face (b) checker board (c) circle pattern

Figure 4 Visualization of conformality using texture mapping in computer graphics.

2.2 Conformal representation of multi-holed annulus

Figure 5 shows the conformal mappings of a multi-holed annulus. The planar domains are circular disks with circular holes. If we specify one boundary of the surface to be mapped to the unit circle, then all such a mapping is unique up to Möbius transformations. Multi-holed annulus can also be conformally mapped to an annulus with concentric circular arcs as shown in the figure 5. The planar domains are determined by the conformal structure of the original surface.

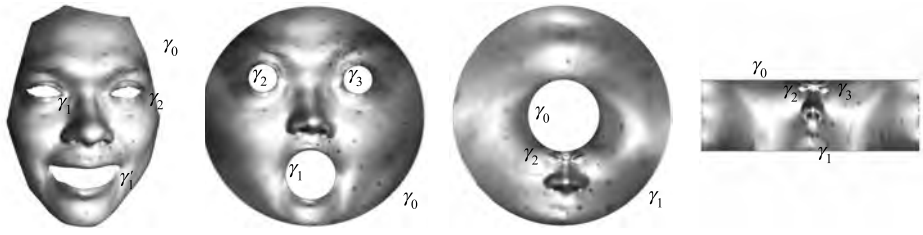

Figure 5 Conformal mappings of a multi-holed annulus.

2.3 Holomorphic differentials

On a Riemann surface, the derivative of a holomorphic function is called a *holomorphic differential*. Let S be a Riemann surface with a conformal atlas $\{(U_\alpha, \phi_\alpha)\}$ and ω is a differential form. On each local chart (U_α, ϕ_α), suppose z_α is the local complex coordinates, then

$$\omega = f(z_\alpha)dz_\alpha,$$

where $f(z_\alpha)$ is a holomorphic function, then ω is called a *holomorphic 1-form*. The real and imaginary components of ω are real *harmonic 1-forms*, which are conjugate to each other. According to Hodge theorem, each cohomology class has a unique harmonic form.

The holomorphic 1-forms can be visualized using the same technique as the visualization of conformal mapping. By integrating the holomorphic differentials, we can locally map the surface to the plane, the mapping is conformal and visualized by checker board texture mapping.

Figure 6 shows the holomorphic differentials on the animal surfaces. Figure 7 shows the holomorphic differentials on the Michelangelo's David surface.

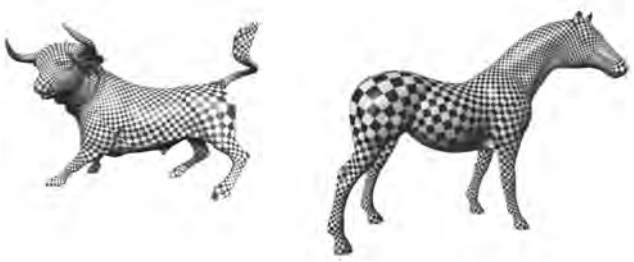

Figure 6 Visualization of holomorphic differentials on animal surfaces.

Figure 7 Visualization of holomorphic differentials on Michelangelo's David.

2.4 Riemann uniformization

Riemann uniformization theorem states that all surfaces in real life can be conformally mapped to three canonical shapes: the unit sphere, the Euclidean plane and the hyperbolic space. Namely, all surfaces admit one of the three canonical geometries, spherical, Euclidean or hyperbolic geometry. It can also be interpreted as all surfaces admit a canonical Riemannian metric, which is conformal to the original metric and induces constant Gaussian curvature, which is $+1$, 0 or -1. Such a metric is called the *uniformization metric* of the surface.

Figure 8 illustrates the uniformization theorem. Closed surfaces without any handle as shown in the first column can be conformally mapped to the unit sphere. Closed surfaces with one handle can be periodically mapped to the plane. For example, the whole kitten surface in the middle column of the figure can be conformally mapped to a parallelogram on the plane, the repetition of the parallelogram forms a tiling of the whole plane. The third column shows an exotic bottle, which has two handles. The surface has no self-intersection and is embedded in $\mathbb{R}^3$. It can be conformally periodically mapped to the unit disk, which represents the hyperbolic space. The whole surface is mapped to a hyperbolic octagon, the repetition of the octagon forms a tiling of the whole hyperbolic space.

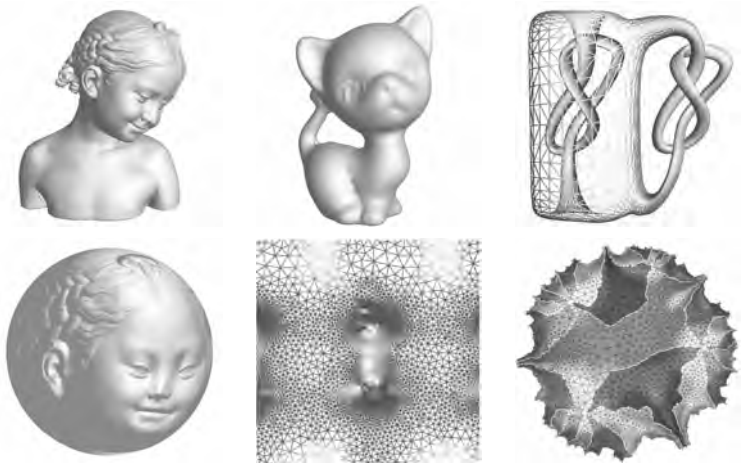

(a) $\chi > 0$ (b) $\chi = 0$ (c) $\chi < 0$

Figure 8 Uniformization Theorem: all surfaces with Riemannian metric can be conformally embedded onto three canonical spaces: the sphere, plane and hyperbolic space.

Suppose $\mathbf{g}$ is the Riemannian metric on the surface S, then *normalized surface Ricci flow* can deform the metric conformally to the uniformization metric

$$\frac{du(t)}{dt} = -2(K(t) - 2\pi\frac{\chi(S)}{A(t)}), \tag{2.1}$$

where $\chi(S)$ is the Euler characteristic of S, $A(t)$ is the area of the Riemannian metric $\mathbf{g}(t)$.

It is easy to see that the area under $\mathbf{g}(t)$ are preserved. The Gaussian curvature evolves like a heat diffusion process.

2.5 Teichmüller space

Surfaces can be classified using conformal geometry. Two surfaces are conformally equivalent, if they can be conformally mapped to each other. It is challenging to verify if two surfaces are conformal equivalent. Roughly speaking, for closed surfaces with one handle, if the shapes of the parallelograms are similar, then they are conformally equivalent. The same result holds for surfaces with more handles. For closed surfaces with two handles, if their hyperbolic octagon are congruent in the hyperbolic space, then they are conformally equivalent.

The conformal equivalence classes form a finite dimensional space, which is called the Modular space, which is the space of shapes. The universal covering space of the modular space is the Teichmüller space, which has simpler topology and is easier to handle. Each point in the shape space represents a shape, each curve represents a deformation process.

Surface classification using conformal structures is described in [2]. The methods for computing general geometric structures are in [4]. Shape space application using Ricci flow is described in [5]. Discrete surface Ricci flow methods are described in [20].

2.6 General geometric structure

Suppose X is a topological space, G is the transformation group of X, a (X,G) *structure* of a surface S is an atlas, such that the local coordinates are in X, the transition functions are in G. For example, a spherical structure is an atlas, where all the local coordinates are on the sphere, all the transition functions are rotations. The three frames in figure 8 can be interpreted as the visualization of spherical structure, Euclidean structure and the hyperbolic structure respectively.

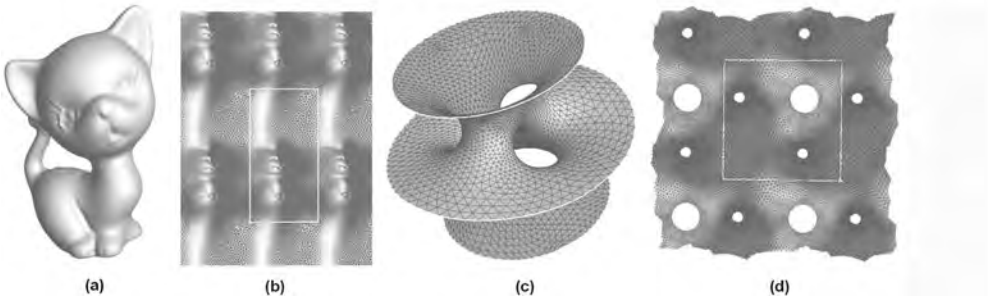

Figure 9 Visualization of the affine structures of two genus one surfaces.

If a surface admits a (X,G) structure, then the corresponding geometry can be defined on the surface directly. For example, in the automobile industry and mechanics engineering fields, surfaces are represented as splines, which are piecewise rational polynomials. Conventional splines are defined on the Euclidean plane and constructed based

on affine invariants. The fundamental problem in the computer aided geometric design (CAGD) field is to construct splines defined on arbitrary surfaces. If the surface admits an *affine structure*, then splines can be defined on the surface without any difficulty. Unfortunately, very few surfaces admit affine structure. This fact causes intrinsic difficulty for applications in the CAGD/CAD field. But fortunately, all surfaces admit *real projective structure*. How to construct splines based on real projective geometry is an active research area in geometric modeling today. Figure 10 visualizes the hyperbolic and real projective structures of a genus two surface.

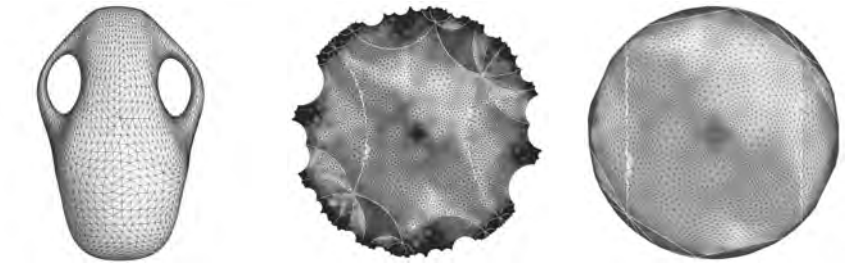

Figure 10 Visualization of the hyperbolic structure and the real projective structure of a genus two vase model.

3 Algorithms for computing conformal mappings

We summarize the major algorithms for computing conformal mappings of surfaces with various topologies.

3.1 Harmonic maps for topological spheres

The harmonic map between a topological sphere and the canonical unit sphere is automatically conformal. The computational algorithm is based on non-linear heat diffusion process. We first construct a degree one map, such as the Gauss map, then we compute the Laplacian of the map, and update the map along the negative direction along the tangential component of the Laplacian. Because of the projection to the tangential space, the heat diffusion process becomes non-linear. Different solutions differ by Möbius transformations of the sphere. Therefore, normalization conditions are necessary. Figure 19 shows one example of conformal mapping of a topological sphere.

Figure 11 Harmonic maps for topologoical spheres.

3.2 Riemann mappings of topological disks

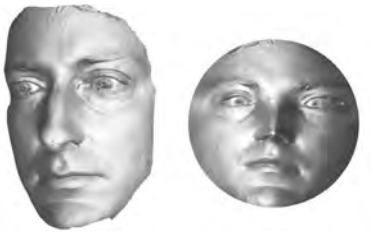

Figure 12 Riemann mapping.

Harmonic maps between a topological disk to the unit disk may not necessarily be conformal. We compute the double covering of a topological disk, which is a topological sphere, then we compute a conformal map between the doubled surface and the unit sphere, such that each copy of the topological disk is mapped to a hemisphere. Then we use stereo-graphic to project the unit sphere onto the whole plane, the lower hemi-sphere is mapped to the unit disk. This induces the Riemann mapping from the surface to the unit disk.

3.3 Conformal mappings with free boundaries

Figure 13 Solving Beltrami equation using free boundary condition.

Conformal mappings with free boundaries can be achieved by discrete approximation of Beltrami equation, a special case is the Riemann-Cauchy equation. The advantage of this method is that it is linear and efficient. The disadvantage is the less control of the boundaries. It mainly handles genus zero surfaces. The mapping results may have self-overlapping. Extra constraints can be added to enhance the mapping result, such as feature point or feature curves.

3.4 Conformal mapping of multi-holed annuli

Figure 14 Conformal Mapping between a multi-holed annulus to a unit disk with circular holes.

If the input surface is an annulus with multiple holes, the conformal mapping is more complicated to compute. It can be mapped onto the unit disk with circular holes. In each homotopy class of degree one mappings, such kind of mapping exists and is unique upto Möbius transformation. We apply the Euclidean Ricci flow method to construct such kind of mapping. The centers of the circles and the radii of the circles are conformal invariants and determined by the geometry of the input surface.

3.5 Holomorophic 1-forms

All metric surfaces are Riemann surfaces, which admit holomorphic 1-forms. The group of the holomorphic 1-forms has special structure, the generators can be explicitly calculated. A holomorphic 1-form has zero points, the number of zero points equals to the absolution value of the Euler number. In the neighborhood of normal points, holomorphic 1-form induces conformal maps between the neighborhood to the complex domains. Isoparametric curves through zero points can be used to segment the surface. Figure 15 illustrates a conformal texture mapping induced by a holomorphic 1-form.

Figure 15 Conformal texture mapping induced by a holomorphic 1-form.

3.6 Conformal mapping of multi-holed annuli to annulus with concentric circular arcs

Special holomorphic 1-forms can be constructed on a multi-holed annulus, such that the whole surface is mapped to an annulus with concentric circular arcs. Two boundaries are mapped to the inner and the outer boundaries of the annulus, other boundaries are mapped to the slits. Computing such holomorphic 1-forms is a linear problem, and the most difficult part is to find harmonic 1-forms. Figure **??** shows the conformal mapping of a three-holed face surface, (the mouth is open), the target domain is a unit disk with two concentric circular arcs. The exterior boundary of the face is mapped to the outer circle of the annulus, the mouth boundary is mapped to the inner circle. The boundaries of eyes are mapped to the two circular slits. Then we conformally mapped the annulus to the rectangle, the outer and inner circles are mapped to parallel lines and the boundaries of eyes are mapped to horizontal slits.

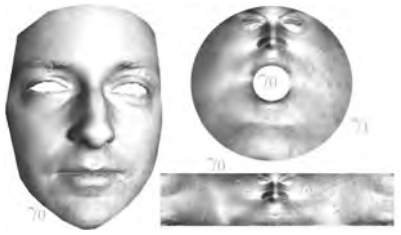

Figure 16 Conformal Mapping between a multi-holed annulus to an annulus with concentric circular arcs and a rectangle with slits.

3.7 Euclidean ricci flow for genus one surface

Euclidean Ricci flow method computes special metrics of the surface conformal to the original metric with prescribed target curvature. For genus one closed surfaces, we set the target Gaussian curvature to be zero everywhere. The universal covering space of the surface can be isometrically embedded on the plane. Figure 17 shows one example. The kitten surface is of genus one, the universal covering space is embedded on the plane. The rectangle is a fundamental polygon.

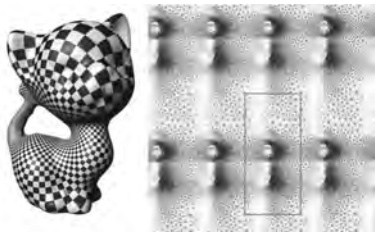

Figure 17 Conformal flat metric of a genus one surface, computed using Euclidean Ricci flow.

3.8 Hyperbolic ricci flow for high genus surface

Figure 18 Conformal hyperbolic mapping of a genus two surface.

For high genus surfaces, there exists a unique Riemannian metric, which is conformal to the original Riemannian metric, and induces constant Gaussian curvature everywhere, the constant is -1. Such kind of metric can be computed using hyperbolic Ricci flow. The universal covering space of the surface can be isometrically embedded on the hyperbolic space. Figure **??** demonstrates the embedding of the universal covering space of a genus two surface on the Poincaré model of hyperbolic space.

3.9 Conformal metric designed by a prescribed curvature

The conformal metrics and the curvatures of a surface are essentially of one-to-one correspondence. The conformal metric can be computed using a prescribed curvature on the surface using Euclidean Ricci flow method. Figure 19 shows one example. The input surface is a topological disk. It is mapped to the planar domains specified by curvature on the boundaries. The curvature of interior points are zero everywhere. The conformal mapping induced by the metric is fully controlled by the prescribed boundary curvatures.

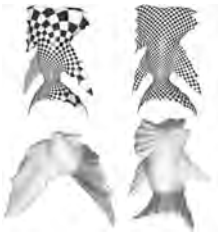

Figure 19 Conformal flat metrics are designed by the target curvature.

4 Applications

Computational conformal geometric methods are valuable for a broad range application in geometric modeling, computer graphics, computer vision, visualization, medical imaging and scientific computing and many other engineering fields.

Computational conformal geometric methods have the following merits: All surfaces in daily life are Riemann surfaces and admit conformal structures. All surfaces, no matter how complicated the shape is, can be conformally deformed to three canonical shapes. For example, all genus zero surfaces can be mapped to the unit sphere, preserving the conformal structures. In practice, conformal geometric methods are suitable to efficiently handle large deformations. Conformal geometric methods are equivalent to solve an elliptic PDE, therefore they are stable and robust.

The followings are some examples of direct applications.

4.1 Computer graphics

Conformal geometry has numerous applications in computer graphics, including surface parameterization, mesh repairing, texture mapping and synthesis, surface re-meshing,

mesh matching, mesh-spline conversion, geometric morphing, efficient rendering, animation and many other applications.

Surface Parameterizations In computer graphics, surface parameterizations refer to the process of mapping the surface onto $2D$ planar domains. The mapping will unavoidably introduce distortions, which can be further classified to *area distortion* and *angle distortion*. It is impossible to eliminate both area distortion and angle distortion, unless the shape is flat. Conformal geometric methods can completely eliminate angle distortions.

The basic process is to construct a conformal map from the surface to the plane. In practice, we can add other constraints for the mapping. For example, we prescribe the images of some feature points, or the target positions of some curve land marks; we can enlarge the size of the image of some part of the surface and shrink the other; we can require area distortion of the mappings to as uniform as possible, etc.

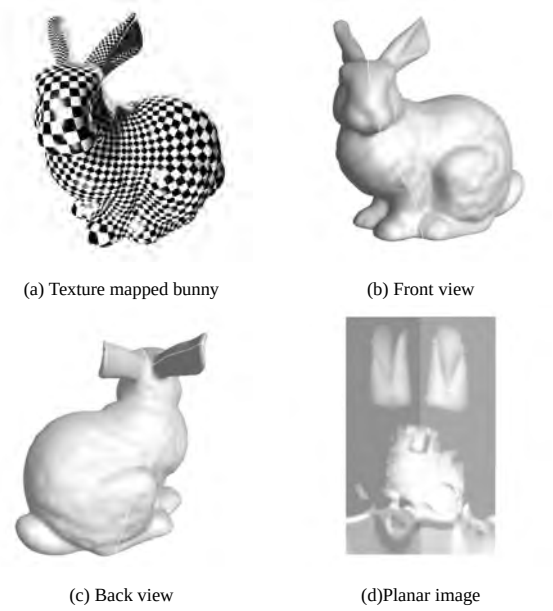

(a) Texture mapped bunny (b) Front view

(c) Back view (d)Planar image

Figure 20 Conformal parameterization of Stanford bunny model.

Figure 20 illustrates the process. We first construct a conformal mapping to map the Standford bunny surface shown in (b) and (c) to the planar domain shown in (d), which is called the texture domain. In order to improve parameterization quality on the two ears, we have carefully designed the mapping. The left part and the right part of the bunny are maps to two rectangles. We preserve the normal information on the planar image (d). So we can see the correspondence between the surface and the image. Globally, the sizes of different parts are changed drastically. This also demonstrates that conformal mapping locally can be treated as scalings. The area distortions can be predicted by the Gaussian curvature of the surface and the relation between the area distortion function and the

Gaussian curvature function can be accurately formulated and solved using surface Ricci flow method.

The global conformal surface parameterization algorithms based on Riemann surface theory can be found in [6]. Algorithms for computing conformal structures are explained in [7] and [8].Optimal conformal surface parameterizations based on conformal structure is described in [9].

(a) Geometry (b) Texture mapping

Figure 21 Texture mapping using hyperbolic parameterization.

Texture Mapping In computer graphics, surfaces are approximated by triangular meshes, which can be supported by graphics hardware directly. The rendering efficiency of the hardware depends on the resolution of the mesh. For real time applications, usually low resolution meshes are preferred. Small geometric details, and material properties are modeled as texture images. The paramterization process maps each vertex to the planar domain, and obtains its $2D$ coordinates, which is called the texture coordinates. Then graphics hardware will glue the texture to the meshes using the texture coordinates. Figure 21 illustrates the process.

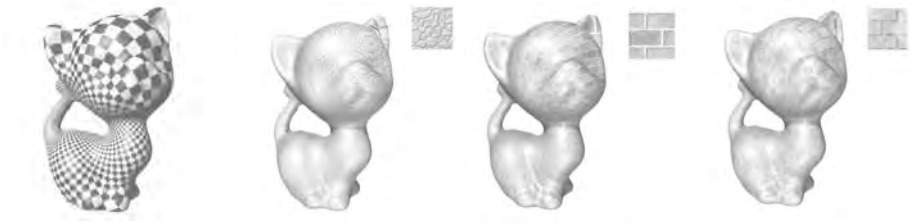

Figure 22 Conformal texture mapping of a genus one closed surface.

Figure 22 shows texture mappings of the genus one kitten surface. Different textures are illustrated as the upper right corners, the conformal parameterization is demonstrated by checker board texture mapping on the left.

Figure 23 Texture synthesis using conformal parameterization [10].

Texture Synthesis Figure 23 demonstrates a texture synthesis application of conformal parameterization. Given a small patch of texture sample, texture synthesis process generates large texture to cover the whole surface. Instead of generating new texture in 3*D* on the surface directly, we generate the texture on the 2*D* parameter plane. By using conformal parameterization, the local shape of the texture will not be distorted. Therefore, the synthesis algorithm solely focuses on the size of the local shape. It is much more efficient to generate uniform textures. The work on uniform texture synthesis based on conformal structure is explained in [10].

Figure 24 Geometric morphing of the Standford bunny surface to the unit sphere.

Geometric Morphing Figure 24 shows a geometric morphing process using the conformal mapping technique. The Standford bunny surface S is a topological sphere, which can be conformally mapped to the unit sphere $\mathbf{S}^2$, we denote the mapping as $\phi : S \to \mathbb{S}^2$. Then we can construct a family of surfaces to deform from the bunny to the sphere. The simplest morphing is the linear combination of the initial shape and the target shape. More complicated morphing sequence can be constructed similarly. The conformal mapping is computed using non-linear harmonic map method.

Geometry Images General meshes have both connectivity information of the triangulations and geometric information represented as the coordinates of the vertices. After re-meshing, the quad-mesh connectivity is regular. It is not necessary to encode the connectivity any more; we just record the coordinates of vertices. We can color encode the coordinates and represent a surface as an image, which is called geometry image. There are two pipelines in graphics hardware, one handles meshes and the other handles texture images. Geometry image unifies both geometry and texture, which has the potential to simplify the graphics hardware. Geometry images can be applied to efficient rendering. Figure 25 shows a geometry image for Michelangelo's David head model. The details of geometry image are presented in [11].

(a) Original Surface (b) Conformal Parameterization (c) Geometry Image (d) Normal map

Figure 25 Geometry image of Michelangelo's David head model.

4.2 Computer vision

Conformal geometry has been applied in computer vision for surface matching, shape comparison, shape classification, geometric analysis and tracking.

Surface Matching Surface matching is a fundamental task for computer vision, graphics and medical imaging. Figure 26 shows the basic idea of using conformal mappings to convert $3D$ matching problems to $2D$ ones. Suppose S_1 and S_2 are two surfaces in $\mathbb{R}^3$. $\phi_1 : S_1 \to \mathbb{D}$ and $\phi_2 : S_2 \to \mathbb{D}$ are conformal mappings to map surfaces to the canonical planar domain. $\bar{f} : \mathbb{D} \to \mathbb{D}$ is a a map from D to itself, this is a $2D$ matching process. Then

$$f = \phi_2^{-1} \circ \bar{f} \circ \phi_1, S_1 \to S_2,$$

is the desired $3D$ matching.

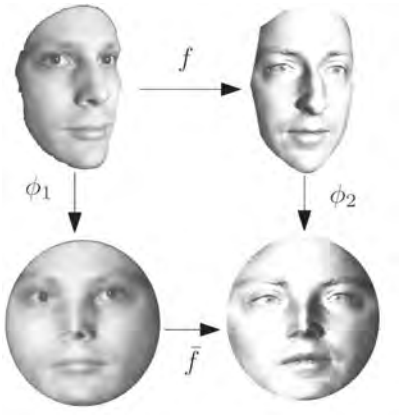

Figure 26 Surface matching using conformal mapping.

Figure 27 demonstrates the fact that isometric deformation preserves the conformal structure. The original surface in (a) is a plastic mask, which can only be bent and can hardly be stretched. We deform it to get another surface shown in (c). We use $3D$ scanner to acquire their shapes, denoted as S_1 and S_2. Then we use conformal map $\phi_1 : S_1 \to \mathbb{R}^2$ and $\phi_2 : S_2 \to \mathbb{R}^2$ with the constraint that the images of all the boundaries are circles. We

(a) Original surface (b) Planar image of (b) (c) Deformed surface (d) Planar image of (c)

Figure 27 Isometric deformation from (a) to (c) preserves conformal structures, their planar images of conformal mappings are consistent shown in (b) and (d). Courtesy of Dimitris Samaras [12].

do not specify the centers and radii of the images of the boundaries, they are calculated automatically by our conformal geometric algorithms. Their planar images are shown in (b) and (d), which are identical. Then the $2D$ map $\bar{f}$ is the identity of the two hole annulus, the $3D$ map $f = \phi_2^{-1} \circ \bar{f} \circ \phi_1$, which is exactly the isometric deformation. This example shows that conformal geometric methods can recover isometric maps automatically. Therefore, for the purpose of surface matching, conformal geometric methods reduce the dimensionality and recover isometric maps, furthermore, they can handle surfaces with arbitrary topologies.

Figure 28 Surface matching between two high genus surfaces using conformal geometric methods.

In figure 28, we matched two genus two surfaces. We visualize the matching by transferring the textures from the domain surfaces to the range surfaces. Figure 29 shows the surface matching between two genus two surface by a geometric morphing.

Figure 29 Visualization of surface matching by surface morphing.

Surface matching with exact feature alignment is in [13].$3D$ surface matching, recognition and stitching using conformal geometry is described [14].

(a) (b) (c) (d) (e)

Figure 30 **Snapshots from a Tracking Sequence of Subject A:** a) Initial data frame. b) Initial tracked frame. c) Data at the expression peak. d) Tracked data at the peak. e) Close-up at the peak. [12].

Surface Tracking Tracking dynamic shapes with large deformation is a challenging task. By using conformal geometric methods, 3D surfaces are mapped onto 2D domains, and dynamic surfaces can be consistently matched. Major feature points are aligned and tracked. Figure 30 illustrates such an example. We match a generic face mesh to real facial data sets acquired using high speed 3D scanner.

We performed tracking on four subjects performing various expressions for a total of twelve sequences of $250-300$ frames each (at 30Hz). Each frame contains approximately $80K$ 3D points, whereas the generic face mesh contains 8K nodes. Our technique tracks very accurately even in the case of topology change. Details of high resolution tracking of non-rigid $3D$ motion are presented in [12].

Shape Space Surfaces can be classified by conformal equivalence. For closed surfaces with one handle (genus one), all conformal classes form a 2 dimensional space, namely, each conformal class can be represented by 2 real parameters. For genus $g > 1$ closed surfaces, all the conformal equivalent classes form a $6g-6$ dimensional space, which is called the Teichmüller space. The *Teichmüller Coordinates* of a surface can be explicitly computed and as the fingerprint of the shape, which can be applied to geometric database indexing and the shape comparison purposes.

Given a pair of topological pants (a topological annulus with two holes), we can compute a unique hyperbolic metric and embed it in the hyperbolic space. The Teichmüller coordinates of it are the geodesic lengths of three boundaries under the hyperbolic metric. Figure 31 shows three such kind of surfaces and their embedding in the hyperbolic space. If the fundamental polygons are congruent in the hyperbolic space, the corresponding surfaces are conformally equivalent. It is easy to see that every surface in the figure is not conformal equivalent to any other one.

The similar idea can be applied to surfaces with more complicated topologies. Figure **??** shows the fundamental polygons of two genus two surfaces in the hyperbolic space. Because these hyperbolic polygons are not congruent, there is no conformal mapping between the two surfaces (in the given homotopy class). Figure 33 shows the fundamental polygons of two genus three surfaces in the hyperbolic space, one is the sculpture model, the other is Michelangelo's David. They are not conformal equivalent either. Shape classification using conformal invariants has the potential to index large scale geometric database.

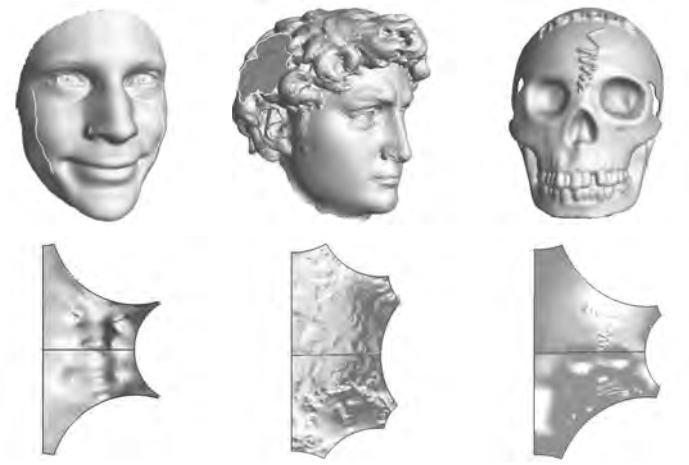

Figure 31 The coordinates of topological annuli with 2 holes in the shape space are the lengths of their boundaries under the hyperbolic metric. The shape of their fundamental polygon indicates the shape space coordinates.

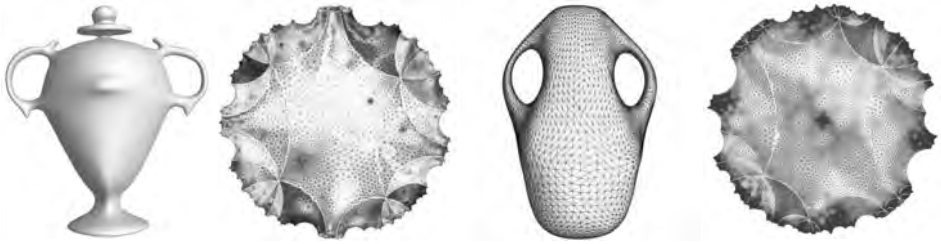

Figure 32 The shape of the fundamental polygon determines the conformal class of the surface. The two genus two surfaces in the figure are not conformal equivalent.

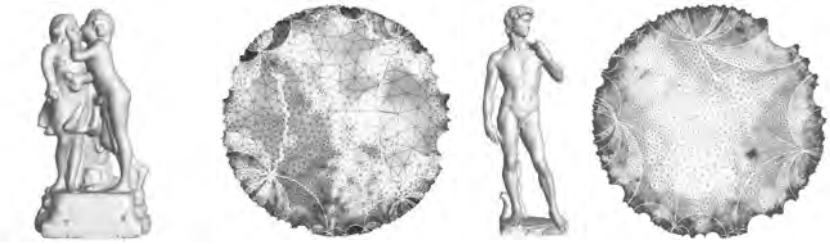

Figure 33 The shape of the fundamental polygon determines the conformal class of the surface. The two genus three surfaces in the figure are not conformal equivalent.

4.3 Geometric modeling

The surfaces obtained by 3D scanners are represented as point clouds. After geometric processing, triangular meshes are constructed. In geometric modeling fields, surfaces

are usually represented as piecewise polynomials or rational polynomials with higher order continuity, called splines. Conformal geometric method is a useful tool to convert meshes to splines. For the purpose of generalizing splines from planar domain to manifold domain, special atlas needs to be constructed using conformal geometric methods.

Manifold Splines In graphics, surfaces are approximated by piecewise linear polygonal meshes, which are with C^0 continuity. In automobile and manufacturing industries, the requirements for the continuity of surface representations are much higher. In general, a surface representation with C^2 continuity is highly desirable.

Conventional spline schemes are defined on planar domains and based on affine invariants, such as bary-centric coordinates. Therefore, conventional splines are based on affine geometry on the plane. One of the most important properties of a spline scheme is *parametric affine invariance*. This means if we transform the parameters of a spline surface by an affine transformation, preserve the control points of the spline surface, then the shape of the surface does not change.

As we discussed before, if a surface admits an affine structure, then conventional splines can be defined on it. Let M be the domain surface with an atlas $\{(U_\alpha, \phi_\alpha)\}$, the spline will be defined on M. Suppose U_α and U_β intersect each other, the coordinate transition function is given by $\phi_{\alpha\beta} : \phi_\alpha(U_\alpha) \to \phi_\beta(U_\beta)$. Assuem the transition function $\phi_{\alpha\beta}$ is an *affine map* from $\mathbb{R}^2$ to itself. Then we can define conventional splines on the parameter domains $\phi_\alpha(U_\alpha)$ of the local chart (U_α, ϕ_α) , $\phi_\beta(U_\beta)$ of the local chart (U_β, ϕ_β).

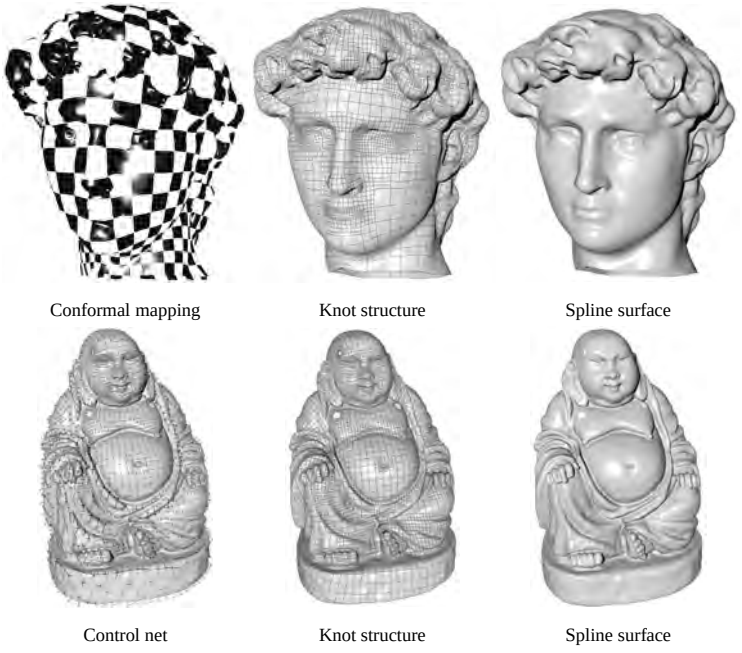

Figure 34 Manifold Splines for Michelangelo's David Head and the Buddha model. [15].

C_α, C_β are the control nets, which are consistent for the overlapping regions. Then by the parametric affine invariance property, the shapes of the spline surfaces defined on the overlapping region are identical. By this way, we can define conventional splines on each local chart and keep the consistencies of the control nets for the overlapping regions. Then the spline surface is coherently defined on the domain manifold M, and resulting spline surface F is with desired continuity.

Therefore, the key is to construct an affine atlas for the domain surface. Any surface with boundaries admits an affine structure and only genus one closed surfaces admit an affine structure. By using conformal geometric methods, affine structures can be explicitly constructed for surfaces with various topologies. Figure 34 shows a manifold T-Spline defined on Michelangelo's David head model and the Buddha model.

The theoretic framework of manifold splines is established in [15]. Then the theory is applied to generalize many spline schemes on manifolds, such as manifold T-Splines, triangular B-Spline, polycube splines. Especially, we construct manifold splines with single singularity [16], which reaches the theoretic limit.

4.4 Medical imaging

With the rapid development of medical imaging technologies, vast medical imaging data are available today. In order to fuse medical images acquired from different modalities, extract surfaces or volumes, register, fuse and compare different geometric data sets, conformal geometric algorithms have been developed and proven to be valuable for real applications.

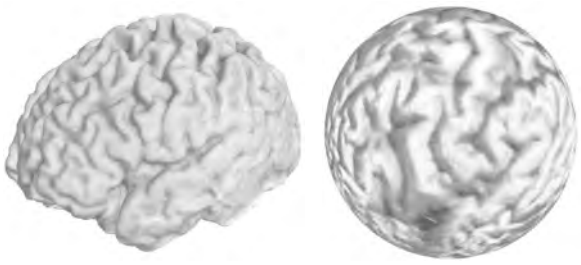

(a) Brain cortex surface (b) Conformal spherical brain mapping

Figure 35 Conformal Brain Mapping.

Conformal Brain Mapping Brain imaging technology has accelerated the collection and databasing of brain maps. Computational problems arise when integrating and comparing brain data. The cortex surface of a brain is highly convoluted and the anatomical structures vary from person to person. One way to analyze and compare brain data is to map them into a canonical space while retaining geometric information on the original cortex surface as far as possible.

Cortical surfaces are of genus zero and therefore can be conformally mapped onto the unit sphere. All such conformal mappings differ by Möbius transformations of the

sphere, which form a 6 dimensional group. For genus zero closed surfaces, harmonic maps are also conformal. We can obtain a conformal mapping by optimizing the harmonic energy. Further constraints are added to ensure that the conformal map is unique. Empirical tests on magnetic resonance imaging (MRI) data show that the mappings preserve angular relationships, are stable in MRIs acquired at different times, and are robust to differences in data triangulation, and resolution. Figure 35 shows the conformal brain mapping of a real human cortical surface.

Conformal brain mapping using nonlinear heat diffusion is introduced in [17]. Conformal brain mapping based on Riemann surface structure is explained in [18].

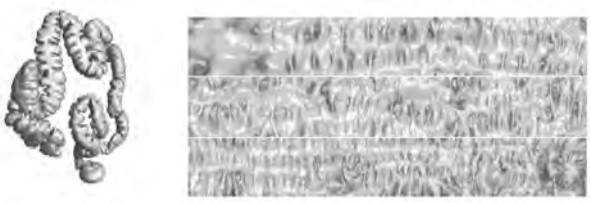

Figure 36 Conformal colon flattening. [19].

Conformal Virtual Colon Flattening Virtual colonoscopy uses computed tomographic (CT) images of patient's abdomen and a virtual fly-through visualization system that allows the physician to navigate within a $3D$ model of the colon searching for polyps, the precursors of cancer. Virtual colonoscopy has been successfully demonstrated to be more convenient and efficient than the real optical colonoscopy. However, because of the length of the colon, inspecting the entire colon wall is time consuming, and prone to errors. Moreover, polyps behind folds may be hidden, which results in incomplete examinations.

Virtual dissection is an efficient visualization technique for polyp detection, in which the entire inner surface of the colon is displayed as a single $2D$ image. We developed a method for colon flattening by computing the conformal structure of the surface, and map the whole colon surface onto a rectangle. The flattening is angle preserving, so the shape of the polyps is preserved. It is convenient for doctors to visually locate the polyps. The colon surface is reconstructed from CT images. We compute its conformal structure and visualize it using checker board texture mapping. The colon surface is a cylinder and can be conformally mapped to the plane periodically, where the boundaries are mapped to parallel lines and each period is a rectangle. We cut the rectangle to three segments. The mapping is conformal, therefore all the geometric details of the colon surface, such as the muscle structure, are preserved on the flattened image. Details of conformal virtual colon flattening can be found in [19].

5 Future works

Computational conformal geometry is an emerging field. There are a lot of challenging open problems both in theory and in practice. Establishing the convergence of discrete

conformal mapping to the smooth solution and estimating the error bounds are widely open. Designing algorithms to compute extremals quasi-conformal maps, designing data structures for holomorphic quadratics are under investigation. Applying computation conformal geometric methods for broader applications and adapt them to real systems is also developing.

Acknowledgements

The work is partially supported by NSF CCF-0448399.We thank Geometric Informatics, Cyberware, Standford, Aim at Shapes for the scanned data sets. We thank all our collaborators in UCLA, Rutgers and State university of New York at stony brook.

References

[1] X. Gu, S. Zhang, R. Martin, P.Huang and S.-T. Yau, Holoimages, *Solid and Physics Modeling*, 2006, pp 129–138.

[2] X. Gu and S.-T. Yau, Surface Classification Using Conformal Structures, *9th IEEE International Conference on Computer Vision ICCV*, 2003, pp 701–708

[3] D. Boley and R. Maier, "A Parallel QR Algorithm for the Non-Symmetric Eigenvalue Algorithm", *in Third SIAM Conference on Applied Linear Algebra*, Madison, WI, 1988, pp. A20.

[4] M. Jin, F. Luo and X. Gu, "Computing General Geometric Structure on Surfaces Using Ricci Flow", *Computer-Aided Design* Vol 39, 2007, No. 8, pp 663–675.

[5] M. Jin, F.Luo, S.-T. Yau and X. Gu, "Computing Geodesic Spectra of Surfaces", *Solid and Physics Modeling* 2007, pp 387–393.

[6] X. Gu and S.-T. Yau, "Global Conformal Parameterization", *Symposium on Geometry Processing*, 2003, pp 127–137.

[7] X. Gu and S.-T. Yau, "Computing Conformal Structures of Surfaces", *Communications in Information and SYstems* vol 2, 2002, No. 2, pp 121-146.

[8] Y. Wang, X. Gu, K.M. Hayashi, T.F.Chan, P.M. Thompson and S.-T. Yau, "Surface Parameterization using Riemann Surface Structure", *ICCV* 2005, pp 1061–1066.

[9] M. Jin, Y. Wang, S.-T. Yan and X. Gu, "Optimal Global Conformal Surface Parameterization", *IEEE Visualization* 2004, pp 267–274.

[10] L. Wang, X. Gu, K. Mueller and S.-T. Yau, "Uniform Texture Synthesis and Texture Mapping Using Global Parameterization", *The Visual Computer* Vol 21, 2005, no. 8-10, pp 801–810.

[11] X. Gu, S.T. Gortler and H. Hoppe, "Geometry Images", *SIGGRAPH* 2002, pp 355–361.

[12] Y. Wang, M. Gupta, S. Zhang, S. Wang, X. Gu, D. Samaras, and P. Huang, "High resolution tracking of non-rigid 3d motion of densely sampled data using harmonic maps", *ICCV*2005, pp 388–395.

[13] C. Carner, M. Jin, X. Gu, and H. Qin, "Topology-driven surface mappings with robust feature alignment", *IEEE Visualization* 2005, pp 69.

[14] S. Wang, Y. Wang, M. Jin, X. Gu, and D. Samaras, "Conformal geometry and its

applications on 3d shape matching, recognition, and stitching", *IEEE Trans. Pattern Anal. Mach. Intell.*, 2007 vol 29, no.7, pp 1209C1220.

[15] X. Gu, Y. He and H. Qin, "Manifold splines", *Graphical Models*, 2006 vol 68, no.3 pp237–254.

[16] X. Gu, Y. He, M. Jin, F. Luo, H. Qin, and S.-T. Yau, "Manifold splines with single extraordinary point", *Solid and Physical Modeling* 2007, pp 61–72.

[17] X. Gu, Y. Wang, T. F. Chan, P. M. Thompson, and S.-T. Yau, "Genus zero surface conformal mapping and its application to brain surface mapping", *IEEE Trans. Med. Imaging* 2004, vol 23 no.8 pp 949–958.

[18] Y. Wang, L. Lui, X. Gu, K. Hayashi, T. Chan, A.W. Toga, P.M. Thompson and S.-T. Yau, "Brain surface conformal parameterization using riemann surface structure", *IEEE Trans. Med. Imaging* 2007, vol 26, no. 6, pp 853–865.

[19] W. Hong, X. Gu, F. Qiu, M. Jin, and A. E. Kaufman, "Conformal virtual colon flattening", *Solid and Physical Modeling* 2006, pp 85–93.

[20] M. Jin, J. Kim and X. Gu, "Discrete surface ricci flow: Theory and applications", *IMA Conference on the Mathematics of Surfaces*, vol. 4647 of Lecture Notes in Computer Science, pp 209C232. Springer, 2007.